Journal of
Mechanics of
Materials and Structures

THERMAL AND MAGNETIC EFFECTS ON THE VIBRATION
OF A CRACKED NANOBEAM EMBEDDED IN AN ELASTIC MEDIUM

Danilo Karličić, Dragan Jovanović, Predrag Kozić and Milan Cajić

msp

msp

THERMAL AND MAGNETIC EFFECTS ON THE VIBRATION
OF A CRACKED NANOBEAM EMBEDDED IN AN ELASTIC MEDIUM

DANILO KARLIČIĆ, DRAGAN JOVANOVIĆ, PREDRAG KOZIĆ AND MILAN CAJIĆ

In this study, we develop a model to describe the free vibration behavior of a cracked nanobeam embedded in an elastic medium by considering the effects of longitudinal magnetic field and temperature change. In order to take into account the small-scale and thermal effects, the Euler–Bernoulli beam theory based on the nonlocal elasticity constitutive relation is reformulated for one-dimensional nanoscale systems. In addition, the effect of a longitudinal magnetic field is introduced by considering the Lorenz magnetic force obtained from the classical Maxwell equation. To develop a model of a cracked nanobeam, we suppose that a nanobeam consists of two segments connected by a rotational spring that is located in the position of the cracked section. The surrounding elastic medium is represented by the Winkler-type elastic foundation. Influences of the nonlocal parameter, stiffness of rotational spring, temperature change and magnetic field on the system frequencies are investigated for two types of boundary conditions. Also, the first four mode shape functions for the considered boundary conditions are shown for various values of the crack position.

1. Introduction

Recently, there has been a growing interest among scientists to study the influence of various multiphysics phenomena on the vibration behavior of nanostructures such as nanorods [Murmu et al. 2014; Alper and Hamad-Schifferli 2010; Martín et al. 2012], nanobeams [Kiani 2012; Youssef and Elsibai 2011; Firouz-Abadi and Hosseinian 2012], nanoplates [Murmu et al. 2013; Arani et al. 2013; Kiani 2014a; A. Haghshenas and Arani 2013], etc. Often, such studies are related to the application of nanostructures in nanoelectromechanical systems (NEMS) [Batra et al. 2007; Popov et al. 2007]. Understanding the dynamic behavior of such systems is of prime importance in design procedures and the practical application of NEMS devices. Materials such as carbon, zinc-oxide, gold, silver and boron-nitride nanotubes [Xie et al. 2000; 2004; Wu et al. 2005; Yum and Yu 2006] and also graphene sheets [Gómez-Navarro et al. 2008; Schniepp et al. 2006; Niyogi et al. 2006] have superior mechanical, physical and thermal properties, which have lately become very important in nanoengineering practice. For the analysis of nanostructures, there are three basic approaches: experimental analysis [Meyer et al. 2007; Jensen 1999], molecular dynamic simulation [Park et al. 2005; Bershtein et al. 2002] and the continuum mechanics approach [Eringen 1972; 1983; Reddy and Pang 2008; Ansari et al. 2012; Jam et al. 2012]. Experimental studies of nanostructures are very important for determining their physical properties. However, direct measurement of properties is difficult due to very small dimensions of structures and weak control of

experimental parameters, which makes this approach very expensive. On the other hand, molecular dynamics is a highly developed method to simulate the dynamic behavior of nanostructures. However, this approach is applicable only to nanostructures with a small number of atoms and molecules whereas for large-sized nanoscale systems, such as nanocomposites and multiple nanostructure systems, it is time-consuming and computationally prohibitive. All this leads to the conclusion that continuum-based theories need to be considered. Since the mechanical behavior of nanostructures strongly depends on the size effects when the system is very small compared to the molecular distances, classical continuum theories need to be modified in order to consider small-scale effects. In the nonlocal theory of Eringen, small-scale effects are introduced into a constitutive equation via a single material parameter. The main assumption of this theory is that the stress at a point is a function of strains at all other points in the continuum body. According to Eringen [1972; 1983], the excellent approximation can be provided for a large class of multiphysics phenomena with internal length scale ranging from the atomistic to the macroscopic scale. Thus, using the classical continuum theory and ignoring the small-scale effects and atomic forces when analyzing the nanostructures may lead to inaccurate results and hence erroneous designs.

In recent years, a large number of researchers have investigated the influence of different physical effects on the dynamic behavior of one-dimensional nanostructures. Murmu and Pradhan [2009] investigated the influence of thermal and nonlocal effects on the free vibration of a single-walled carbon nanotube (CNT) embedded in an elastic medium. In [Murmu and Pradhan 2010], they also examined the stability of CNT in an elastic medium under the influence of temperature change. In both cases, they used nonlocal Euler–Bernoulli beam theory. Benzair et al. [2008] reformulated the classical Timoshenko beam theory by using the nonlocal elasticity. In addition, they introduced thermal effects through the constitutive relation for vibration analysis of CNT. In [Ke and Wang 2012], governing equations of motion were derived by using the Hamilton principle and nonlocal elasticity for thermoelectromechanical vibration of the piezoelectric nanobeams with various boundary conditions. In addition, they investigated the influence of the nonlocal parameter, temperature change, external electric voltage and axial force on the thermoelectromechanical vibration characteristics of the piezoelectric nanobeams. Hosseini-Hashemi et al. [2014] considered surface effects on the free vibration of piezoelectric functionally graded nanobeams by using the nonlocal elasticity theory. Further, they investigated the influences of the surface and nonlocal effects on the piezoelectric field and the static and dynamic behavior of the nanobeam. Kiani [2014b] investigated the influence of a three-dimensional magnetic field on the vibration and instability of a single-walled CNT. The equations of motion were obtained from the nonlocal Rayleigh beam theory and Maxwell equations. In addition, the author derived an expression for a critical transverse magnetic field associated with the lateral buckling of the single-walled CNT. Li et al. [2011] obtained coupled dynamic equations of multiwalled CNTs subjected to a transverse magnetic field by considering the Lorentz magnetic forces. In addition, they showed the influence of van der Waals force on the dynamic characteristics of multiwalled CNTs. Further, they examined the effects of the van der Waals forces on vibration characteristics of a multiwalled CNT under a transverse magnetic field, where the CNT was represented by a cylindrical shell. Wei and Wang [2004] investigated the wave propagation in a single-wall carbon nanotube for two different propagating modes, i.e., the transverse electric and transverse magnetic modes. Recently, Karličić et al. [2014] studied the influence of an axial magnetic field on vibration of multiple coupled viscoelastic CNTs embedded in a viscoelastic medium. The authors

determined complex and critical values of natural frequencies of the system and performed a detailed parametric study.

The study of the vibration behavior of cracked CNTs is of great theoretical and practical interest for better understanding of the mechanical response of nanostructures. Based on a growing number of experimental studies, it was found that the CNT is not a perfect nanostructure as it seems at the beginning of investigations. Different types of defects cause a local change in stiffness of CNTs that may have significant influence on natural frequencies and mode shapes. Moreover, researchers have considered two types of initial defects in carbon nanostructures. In *the first group are topological defects* related to bonds between atoms in an atomic network. This includes Stone–Wales defects [Zhou and Shi 2003; Charlier 2002] causing irregularities in the hexagonal network of carbon-carbon bonds in CNTs, which leads to a disturbance in local stiffness. In *the second group are point defects* related to creating single and multiple vacancies [Charlier 2002; Sammalkorpi et al. 2004; Belytschko et al. 2002] in the atomic network, which leads to degradation of mechanical characteristics of the crystal lattice. In this case, local change in stiffness of CNTs also occurs. From the standpoint of continuum mechanics, this change of local stiffness of CNT can be modeled as a change in the strain energy of a nanobeam. The flexural vibration behavior of a cracked nanobeam based on the nonlocal elasticity theory was investigated by Loya et al. [2009]. They proposed the model of a cracked nanobeam consisting of two segments connected by a rotational spring located at the cracked section. In addition, the authors showed the influence of crack severity, the nonlocal parameter and boundary conditions on natural frequencies of the cracked nanobeam. Torabi and Dastgerdi [2012] investigated the free vibration of a cracked nanobeam modeled via nonlocal elasticity and Timoshenko beam theory, where the cracked nanobeam is represented by two segments connected by a rotational spring. They analyzed the effects of crack position, ratio and the nonlocal parameter on the vibration mode and frequency parameter. The bending vibrations of a cracked nanobeam with surface effects were studied in [Hasheminejad et al. 2011]. In [Yang and Chen 2008], the free vibration and stability of the beam made of functionally graded materials containing an open crack were investigated by using Euler–Bernoulli beam theory and the rotational spring model at the cracked section. Roostai and Haghpanahi [2014] discussed the vibration behavior of a nanobeam with multiple cracks for various boundary conditions. They showed the influence of changing the number of cracks on dimensionless frequencies for change in boundary conditions.

As stated in [Yang and Chen 2008], models of cracked nanobeams can be divided into two groups: "continuous" models and "lumped flexibility" models. In this paper, we use the technique that belongs to the method of "lumped flexibility" models, whose main characteristic is that the presence of a crack is modeled via change of the stiffness of beams at the position of the crack, which is equivalent to the stiffness of an inserted spring. The main objective of this paper is to present an analytical model and analyze the vibrational behavior of a cracked nanobeam embedded in an elastic medium by taking into account the magnetic field and thermal effects. In addition, different boundary conditions of the cracked nanobeam are also considered. The governing equation of motion is derived by using the Euler–Bernoulli beam theory, nonlocal thermoelastic constitutive relation and Maxwell relation. The frequency equation is derived and numerically solved for different boundary conditions, and the obtained results are compared to the corresponding ones in the literature. In the parametric study, the effects of various physical parameters on natural frequencies and mode shape functions are also investigated.

2. Problem formulation

2.1. *Nonlocal constitutive relation.* In this subsection, we will provide the fundamental constitutive relation of the nonlocal elasticity and thermoelasticity theory. The basic form of the nonlocal elastic relation for a three-dimensional linear, homogeneous isotropic body is given as

$$\sigma_{ij}(x) = \int \alpha(|x - x'|, \tau) C_{ijkl} \epsilon_{kl}(x') \, dV(x') \quad \text{for all } x \in V, \tag{1a}$$

$$\sigma_{ij,j} = 0, \tag{1b}$$

$$\epsilon_{ij} = \tfrac{1}{2}(u_{i,j} + u_{j,i}), \tag{1c}$$

where C_{ijkl} is the elastic modulus tensor for classical isotropic elasticity; σ_{ij} and ϵ_{ij} are the stress and the strain tensors, respectively, and u_i is the displacement vector. With $\alpha(|x - x'|, \tau)$, we denote the nonlocal modulus or attenuation function, which incorporates nonlocal effects into the constitutive equation at a reference point x produced by the local strain at a source x'. The above absolute value of the difference $|x - x'|$ denotes the Euclidean metric. The parameter $\tau = (e_0 a)/l$, where l is the external characteristic length (crack length and wave length), a describes the internal characteristic length (lattice parameter, granular size and distance between C-C bonds) and e_0 is a constant appropriate to each material that can be identified from atomistic simulations or by using the dispersive curve of the Born–von Kármán model of lattice dynamics. Since it is difficult to use constitutive relations in the integral form for solving practical problems, simplified constitutive relations in the differential form were developed. Based [Eringen 1972; 1983], constitutive relations in the differential form for the one-dimensional case are

$$\sigma_{xx} - \mu \frac{d^2 \sigma_{xx}}{dx^2} = E \epsilon_{xx}, \tag{2a}$$

$$\sigma_{xz} - \mu \frac{d^2 \sigma_{xz}}{dx^2} = G \gamma_{xz}, \tag{2b}$$

where E and G are the elastic modulus and the shear modulus of the beam, respectively; $\mu = (e_0 a)^2$ is the nonlocal parameter (length scales); σ_{xx} and σ_{xz} are the normal and the shear nonlocal stresses, respectively, and $\epsilon_{xx} = u - z \frac{\partial^2 w}{\partial x^2}$ is the axial deformation. Nanomaterials such as CNTs, ZnO nanotubes and other one-dimensional structures are modeled as nanobeams and nanorods by using the nonlocal theory, where internal characteristic lengths ($e_0 a$) are often assumed to be in the range 0–2 nm. When $e_0 a = 0$, the nonlocal constitutive relation is reduced to the classical constitutive relation of the elastic body. The nonlocal thermoelastic constitutive relation model proposed by Zhang et al. [2008] and Murmu and Pradhan [2009; 2010] is a combination of nonlocal elasticity and classical thermoelasticity theory. Therefore, for one-dimensional nonlocal viscoelastic solids, constitutive relations are given by

$$\sigma_{xx} - \mu \frac{d^2 \sigma_{xx}}{dx^2} = E \left(\epsilon_{xx} - \frac{\alpha_x \theta}{1 - 2\nu} \right), \tag{3}$$

where α_x is the coefficient of thermal expansion in the direction of the x axis, ν is the Poisson ratio and θ denotes the change in temperature. If $\theta = 0$, i.e., there is no influence of change in temperature, we then return to the constitutive relation for nonlocal elasticity. It should be noted that Young's modulus of some types of nanomaterials, for example CNT, is insensitive to temperature changes in the tube at

temperatures less than nearly $1100\,\mathrm{K}$, but it decreases at higher temperatures [Hsieh et al. 2006]. In what follows, we will use the constitutive relation for nonlocal thermoelasticity to derive governing equations of motion.

2.2. *Maxwell's relation.*

According to the classical electromagnetic theory [Narendar et al. 2012], the Maxwell equations in differential form are given as

$$J = \nabla \times h, \qquad \nabla \times e = -\eta \frac{\partial h}{\partial t}, \qquad \nabla \cdot h = 0, \tag{4}$$

where J is the current density, h is the distributing vector of the magnetic field, e is the strength vector of the electric fields and η is the magnetic field permeability. In addition, we define the vectors for distributing magnetic field h and electric field e as

$$h = \nabla \times (U \times H), \qquad e = -\eta \left(\frac{\partial U}{\partial t} \times H \right), \tag{5}$$

in which $\nabla = \frac{\partial}{\partial x} i + \frac{\partial}{\partial y} j + \frac{\partial}{\partial z} k$ is the Hamilton operator, $U = (x, y, z)$ is the displacement vector and $H = (H_x, 0, 0)$ is the vector of the longitudinal magnetic field, and (i, j, k) are unit vectors. In the present study, we assume that the longitudinal magnetic field acts on the cracked nanobeam in the axial direction. Now, we can write the vector of the distributing magnetic field in the form

$$h = -H_x \left(\frac{\partial v}{\partial y} + \frac{\partial w}{\partial z} \right) i + H_x \frac{\partial v}{\partial x} j + H_x \frac{\partial w}{\partial x} k. \tag{6}$$

Then, we introduce (6) into the first expressions of (4):

$$J = \nabla \times h = H_x \left(-\frac{\partial^2 v}{\partial x \, \partial z} + \frac{\partial^2 w}{\partial x \, \partial y} \right) i - H_x \left(\frac{\partial^2 v}{\partial y \, \partial z} + \frac{\partial^2 w}{\partial x^2} + \frac{\partial^2 w}{\partial z^2} \right) j + H_x \left(\frac{\partial^2 v}{\partial x^2} + \frac{\partial^2 v}{\partial y^2} + \frac{\partial^2 w}{\partial z \, \partial y} \right) k. \tag{7}$$

Substituting (7) into the expressions for the Lorentz forces induced by the longitudinal magnetic field yields

$$f(f_x, f_y, f_z) = \eta (J \times H) = \eta \left[0i + H_x^2 \left(\frac{\partial^2 v}{\partial x^2} + \frac{\partial^2 v}{\partial y^2} + \frac{\partial^2 w}{\partial z \, \partial y} \right) j + H_x^2 \left(\frac{\partial^2 w}{\partial x^2} + \frac{\partial^2 w}{\partial y^2} + \frac{\partial^2 v}{\partial z \, \partial y} \right) k \right], \tag{8}$$

where f_x, f_y and f_z express the Lorentz force along the x, y and z directions as

$$f_x = 0, \tag{9a}$$

$$f_y = \eta H_x^2 \left(\frac{\partial^2 v}{\partial x^2} + \frac{\partial^2 v}{\partial y^2} + \frac{\partial^2 w}{\partial z \, \partial y} \right), \tag{9b}$$

$$f_z = \eta H_x^2 \left(\frac{\partial^2 w}{\partial x^2} + \frac{\partial^2 w}{\partial y^2} + \frac{\partial^2 v}{\partial z \, \partial y} \right). \tag{9c}$$

In this study, we assume that the displacement of nanobeam $w(x, t)$ and the Lorentz force act only in the z direction, which can be written as

$$f_z = \eta H_x^2 \frac{\partial^2 w}{\partial x^2}. \tag{10}$$

Finally, it is possible to obtain force per unit length of the nanobeam in the form

$$\tilde{q}(x,t) = \int_A f_z \, dA = \eta A H_x^2 \frac{\partial^2 w}{\partial x^2}. \tag{11}$$

2.3. *Mathematical model of a cracked nanobeam.* Zhang et al. [2005] have introduced one type of vacancy defect in CNTs known as a slit defect. Under certain assumptions, the slit defect, resulting from removing C-C atom pairs in the circumferential direction of the regular lattice of CNTs, can be observed as cracks (Figure 1a). Thus, we consider SWCNT with a slit defect, which is embedded in an elastic medium, as a cracked nanobeam by using the nonlocal continuum model with two types of boundary conditions as shown in Figure 1b–d. The cracked nanobeam is represented by two beam segments connected with a rotational spring of stiffness c, where the left segment is before the crack section and the right segment is after the crack section. Both nanobeam segments have the same material properties: Young's modulus E, mass density ρ, cross-section area A, moment of inertia I and the nonlocal parameter μ. Moreover, the nanobeam is under the influence of Lorentz magnetic force induced by the longitudinal magnetic field. These parameters are assumed to be constant along the nanobeam. The nanobeam is considered to be of length L with crack-position L^*. The transversal displacements over the two defined segments of the nanobeam are denoted by $w_1(x,t)$ and $w_2(x,t)$, i.e., the left segment and the right segment, respectively. The nanobeam model is described by using the nonlocal Euler–Bernoulli beam theory, where the effect of the temperature change is introduced through the constitutive relation. The elastic medium is modeled by a Winkler-type elastic foundation, which is represented by
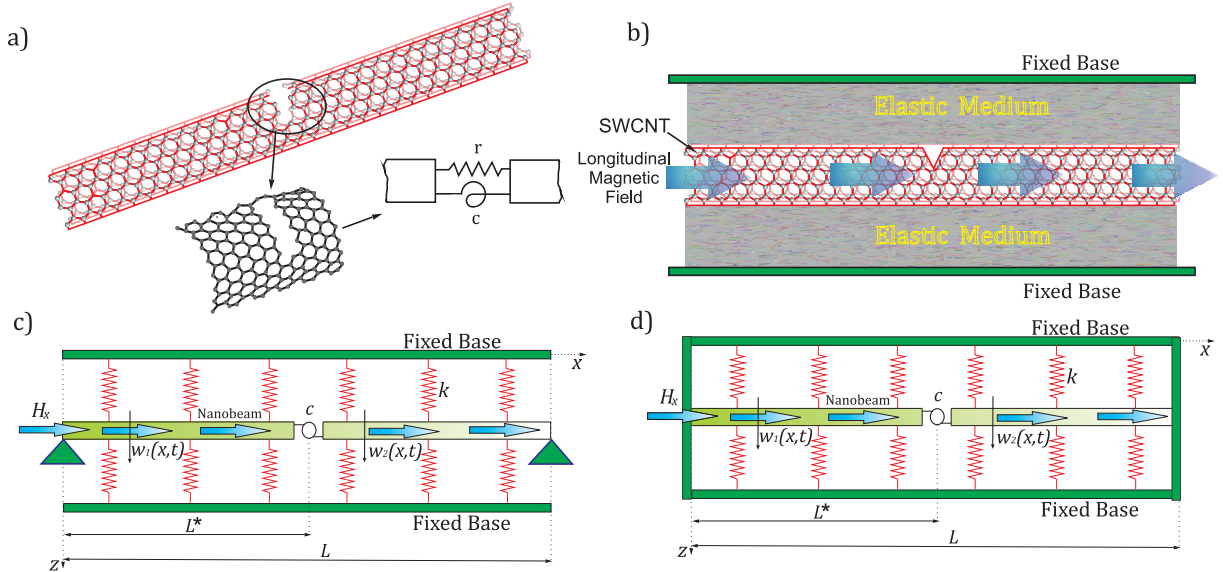
Figure 1. (a) SWCNT with defects. (b) Axial magnetic field exerted on the cracked SWCNT embedded in an elastic medium, physical model; equivalent nonlocal mechanical model of the cracked nanobeam coupled with the Winkler elastic foundation in the axial magnetic field for various boundary conditions. (c) Simply supported. (d) Clamped-clamped.

continuously distributed springs of stiffness k. In the present study, two types of boundary conditions are considered: simply supported (Figure 1c) and clamped-clamped (Figure 1d).

According to Newton's second law, the equilibrium equations for the differential element of the nanobeam can be expressed in the similar manner as in [Kozić et al. 2014], which gives

$$\frac{\partial F_T}{\partial x} - kw + \tilde{q} + N\frac{\partial^2 w}{\partial x^2} = \rho A\frac{\partial^2 w}{\partial t^2}, \tag{12a}$$

$$\frac{\partial N}{\partial x} = \rho A\frac{\partial^2 u}{\partial t^2}, \tag{12b}$$

$$F_T = \frac{\partial M_f}{\partial x}, \tag{12c}$$

where u is the axial displacement and M_f and N are the moment and axial force stress resultants, respectively, defined as

$$M_f = \int_0^A z\sigma_{xx}\,dA, \tag{13a}$$

$$N = \int_0^A \sigma_{xx}\,dA, \tag{13b}$$

where $\tilde{q}$ is the magnetic force per unit length defined in (11).

By using the nonlocal constitutive relation from (3) with expressions (12) and (13) and assuming that the axial displacement u is zero, we can get the equations

$$M_f = \mu\left[kw - \tilde{q} - N\frac{\partial^2 w}{\partial x^2} + \rho A\frac{\partial^2 w}{\partial t^2}\right] - EI\frac{\partial^2 w}{\partial x^2}, \quad i = 1, 2, \tag{14a}$$

$$N = -EA\frac{\alpha_x\theta}{1-2\nu}. \tag{14b}$$

The equation of motion of the nanobeam in terms of transversal displacements $w(x, t)$ is obtained by introducing (14a), (14b) and (12c) into (12a) in the form

$$\rho A\frac{\partial^2 w}{\partial t^2} + kw - \eta AH_x^2\frac{\partial^2 w}{\partial x^2} + EA\frac{\alpha_x\theta}{1-2\nu}\frac{\partial^2 w}{\partial x^2} + EI\frac{\partial^4 w}{\partial x^4}$$
$$= \mu\frac{\partial^2}{\partial x^2}\left[\rho A\frac{\partial^2 w}{\partial t^2} + kw - \eta AH_x^2\frac{\partial^2 w}{\partial x^2} + EA\frac{\alpha_x\theta}{1-2\nu}\frac{\partial^2 w}{\partial x^2}\right] \tag{15}$$

or in the dimensionless form

$$\frac{\partial^2 \overline{w}}{\partial \tau^2} + K\overline{w} + (\overline{N}_\theta - \text{MP})\frac{\partial^2 \overline{w}}{\partial \xi^2} + \frac{\partial^4 \overline{w}}{\partial \xi^4} = \nu^2\frac{\partial^2}{\partial \xi^2}\left[\frac{\partial^2 \overline{w}}{\partial \tau^2} + K\overline{w} + (\overline{N}_\theta - \text{MP})\frac{\partial^2 \overline{w}}{\partial \xi^2}\right], \tag{16a}$$

where

$$\overline{w} = \frac{w}{L}, \qquad \xi = \frac{x}{L}, \qquad K = k\frac{L^4}{EI}, \qquad \text{MP} = \frac{\eta AH_x^2}{EI}L^2,$$
$$\nu^2 = \frac{\mu}{L^2}, \qquad \tau = \frac{t}{L^2}\sqrt{\frac{EI}{\rho A}}, \qquad \overline{N}_\theta = EA\frac{\alpha_x\theta}{1-2\nu}\frac{L^2}{EI}. \tag{16b}$$

K, MP, $\bar{N}_\theta$ and v are the dimensionless spring coefficient, magnetic parameter, thermal axial force and nonlocal parameter, respectively.

Now, we can solve the equation of motion (16a) by assuming the solution is in the form

$$\bar{w}(\xi, \tau) = \sum_{n=1}^{\infty} W_n(\xi)e^{i\Omega_n\tau}, \quad n = 1, 2, 3, \ldots, \tag{17}$$

where $i = \sqrt{-1}$, W_n are the mode functions and Ω_n are the dimensionless natural frequencies for n vibration modes. Introducing the assumed solutions (17) into (16a), we obtain the ordinary differential equation

$$W_n^{\mathrm{IV}}(\xi) + \tilde{b}W_n^{\mathrm{II}}(\xi) - \tilde{c}W_n(\xi) = 0, \tag{18}$$

where $(\cdot)^{\mathrm{I}}$ represents the derivative with respect to ξ and $\tilde{a}$, $\tilde{b}$ and $\tilde{c}$ are constants defined by

$$\tilde{a} = 1 - v^2(\bar{N}_\theta - \mathrm{MP}), \tag{19a}$$

$$\tilde{b} = \frac{\bar{N}_\theta - \mathrm{MP}}{\tilde{a}} + v^2\left(\lambda_n^4 - \frac{K}{\tilde{a}}\right), \tag{19b}$$

$$\tilde{c} = \left(\lambda_n^4 - \frac{K}{\tilde{a}}\right), \tag{19c}$$

$$\lambda_n^4 = \frac{\Omega_n^2}{\tilde{a}}. \tag{19d}$$

Introducing the assumed solutions $W_n(\xi) = \boldsymbol{D}e^{s\xi}$ into (18), we obtain a characteristic equation

$$s^4 + \tilde{b}s^2 - \tilde{c} = 0, \tag{20}$$

where the solutions are given as

$$s_{n1/2} = \pm\sqrt{\frac{-\tilde{b} + \sqrt{\tilde{b}^2 + 4\tilde{c}}}{2}} = \pm\alpha_n, \tag{21a}$$

$$s_{n3/4} = \pm\sqrt{\frac{-\tilde{b} - \sqrt{\tilde{b}^2 + 4\tilde{c}}}{2}} = \pm i\beta_n. \tag{21b}$$

Finally, the general solution of spatial differential equation (18) is written as

$$W_n(\xi) = D_{n1}\sinh(\alpha_n\xi) + D_{n2}\cosh(\alpha_n\xi) + D_{n3}\sin(\beta_n\xi) + D_{n4}\cos(\beta_n\xi), \tag{22}$$

where D_{ni}, $i = 1, 2, 3, 4$, are the unknown constants that are determined from the boundary conditions of the nanobeam.

Now, we consider the case of the nanobeam with a crack, which is located at the distance L^* from the left support, where the term $b = L^*/L$ denotes the dimensionless variable (Figure 1c–d). According to the methodology developed in [Loya et al. 2009; 2006; Fernández-Sáez et al. 1999; Fernández-Sáez and Navarro 2002; Torabi and Dastgerdi 2012], we modeled a cracked nanobeam with two beam segments connected by one linear and one rotational spring positioned at the site of a crack. In this model, we assume that both springs provide additional strain energy in the system caused by the presence of a crack.

Therefore, we obtain total strain energy as the sum of deformation energy of the nanobeam and additional strain energy from the springs in the form

$$U = \frac{1}{2} \int_V (\sigma_{xx} \cdot \epsilon_{xx}) \, dV + \Delta U_c |_{x=L^*}, \tag{23}$$

where σ_{xx} is the stress given by the expression (3), ϵ_{xx} is the axial deformation and ΔU_c is the increment of strain energy. The total strain energy (23) can be written in the expansion form by using (13) as

$$U = \frac{1}{2} \int_V \left(N \frac{\partial u}{\partial x} - M_f \frac{\partial^2 w}{\partial x^2} \right) dV + \left(\tfrac{1}{2} N \Delta u + \tfrac{1}{2} M_f \Delta \theta \right) \big|_{x=L^*}, \tag{24}$$

in which the term $(\tfrac{1}{2} N \Delta u)|_{x=L^*}$ represents the strain energy from a linear spring and $(\tfrac{1}{2} M_f \Delta \theta)|_{x=L^*}$ represents the strain energy from a rotational spring. The relative axial displacement Δu of a linear spring and rotation angle $\Delta \theta$ of the rotational spring, i.e., horizontal displacement and rotation of the edge crack section, are defined as

$$\Delta u = r \frac{\partial u}{\partial x} + k_{NM} \frac{\partial^2 w}{\partial x^2}, \tag{25a}$$

$$\Delta \theta = c \frac{\partial^2 w}{\partial x^2} + k_{MN} \frac{\partial u}{\partial x}, \tag{25b}$$

where r, c, k_{NM} and k_{MN} are the flexibility constants. It should be noted that the constants k_{NM} and k_{MN} represent coupling effects between the axial force and bending moment. In this paper, we analyzed only the free transversal vibrations where the axial displacement is neglected ($u(x, t) = 0$). Because of that, the flexibility constants k_{NM} and k_{MN} are assumed to be small compared to constants c and they are neglected as well [Torabi and Dastgerdi 2012]. Introducing these assumptions into the expression (25), we obtain the axial displacement Δu, angle of rotation $\Delta \theta$ (slope) and increment of the strain energy as

$$\Delta u = 0, \qquad \Delta \theta = c \frac{\partial^2 w}{\partial x^2} = C \frac{\partial^2 \overline{w}}{\partial \xi^2}, \qquad \Delta U_c |_{x=L^*} = \left(\tfrac{1}{2} M_f \Delta \theta \right) \big|_{x=L^*}, \tag{26}$$

where $C = c/L$ is the crack severity or dimensionless flexibility constant [Loya et al. 2009; Torabi and Dastgerdi 2012; Hasheminejad et al. 2011]. In general, flexibility constant C is the function of crack depth and geometry of the cracked section and nanobeam. However, in this analysis, we consider the flexibility constant C as a dimensionless parameter, but its value needs to be determined from the molecular dynamics model [Torabi and Dastgerdi 2012; Kisa and Gurel 2006; Loya et al. 2014]. In addition, it should be emphasized that increment of the strain energy ΔU_c in a cracked nanobeam or other nanostructure could be also determined by using the molecular dynamics model. In this study, values of crack severity are adopted based on the works found in the literature and the main attention is devoted to the investigation of their influence on dynamical behavior of a cracked nanobeam model subjected to the longitudinal magnetic field and temperature change.

Since the cracked nanobeam is modeled as a system of two nanobeams connected in series by a rotational spring, from (16) and (18), we can write the equations for each part of the nanobeam as

$$W_{n1}^{IV}(\xi) + \tilde{b} W_{n1}^{II}(\xi) - \tilde{c} W_{n1}(\xi) = 0, \quad 0 \le \xi \le b, \tag{27a}$$

$$W_{n2}^{IV}(\xi) + \tilde{b} W_{n2}^{II}(\xi) - \tilde{c} W_{n2}(\xi) = 0, \quad b \le \xi \le 1, \tag{27b}$$

where the influence of the crack is given via internal boundary conditions of the system. For such a system of equations, we can write the solution in the form

$$W_{n1}(\xi) = D_{n1} \sinh(\alpha_n \xi) + D_{n2} \cosh(\alpha_n \xi) + D_{n3} \sin(\beta_n \xi) + D_{n4} \cos(\beta_n \xi), \tag{28a}$$

$$W_{n2}(\xi) = D_{n5} \sinh(\alpha_n \xi) + D_{n6} \cosh(\alpha_n \xi) + D_{n7} \sin(\beta_n \xi) + D_{n8} \cos(\beta_n \xi), \tag{28b}$$

where unknown constants D_{ni}, $i = 1, 2, \ldots, 8$, are determined from boundary conditions of the system of nanobeams. In this paper, we consider two types of boundary conditions as shown in Figure 1c–d. They can be mathematically expressed as:

(a) for simply supported boundary conditions (Figure 1c), at $\xi = 0$,

$$\overline{w}_1(0, \tau) = 0 \implies W_{1n}(0) = 0, \tag{29a}$$

$$\overline{M}_{1f}|_{\xi=0} = \left[-\nu^2 \left(\lambda_n^4 - \frac{K}{\tilde{a}} \right) \tilde{a} W_{1n} - \tilde{a} W_{1n}^{II} \right]_{\xi=0} = 0 \tag{29b}$$

and, at $\xi = 1$,

$$\overline{w}_2(1, \tau) = 0 \implies W_{2n}(1) = 0, \tag{30a}$$

$$\overline{M}_{2f}|_{\xi=1} = \left[-\nu^2 \left(\lambda_n^4 - \frac{K}{\tilde{a}} \right) \tilde{a} W_{2n} - \tilde{a} W_{2n}^{II} \right]_{\xi=1} = 0, \tag{30b}$$

(b) for clamped-clamped boundary conditions (Figure 1d), at $\xi = 0$,

$$\overline{w}_1(0, \tau) = 0 \implies W_{1n}(0) = 0, \tag{31a}$$

$$\frac{\partial \overline{w}_1(0, \tau)}{\partial \xi} = 0 \implies W_{1n}^{I}(0) = 0 \tag{31b}$$

and, at $\xi = 1$,

$$\overline{w}_2(1, \tau) = 0 \implies W_{2n}(1) = 0, \tag{32a}$$

$$\frac{\partial \overline{w}_2(1, \tau)}{\partial \xi} = 0 \implies W_{2n}^{I}(1) = 0. \tag{32b}$$

For the crack section ($\xi = b$), we have compatibility conditions that are expressed as

- transversal displacement

$$\overline{w}_2(b, \tau) = \overline{w}_1(b, \tau) \implies W_{2n}(b) = W_{1n}(b), \tag{33a}$$

- bending slope

$$\frac{\partial \overline{w}_2(b, \tau)}{\partial \xi} - \frac{\partial \overline{w}_1(b, \tau)}{\partial \xi} = \Delta\theta \implies W_{2n}^{I}(b) - W_{1n}^{I}(b) = C W_{1n}^{II}(b), \tag{33b}$$

- bending moment

$$\overline{M}_{1f}|_{\xi=b} = \overline{M}_{2f}|_{\xi=b}$$

$$\Longrightarrow \left[-\nu^2 \left(\lambda_n^4 - \frac{K}{\tilde{a}} \right) \tilde{a} W_{2n} - \tilde{a} W_{2n}^{\mathrm{II}} \right]_{\xi=b} = \left[-\nu^2 \left(\lambda_n^4 - \frac{K}{\tilde{a}} \right) \tilde{a} W_{1n} - \tilde{a} W_{1n}^{\mathrm{II}} \right]_{\xi=b}, \quad (34a)$$

- transversal force

$$\overline{F}_{1T}|_{\xi=b} = \overline{F}_{2T}|_{\xi=b}$$

$$\Longrightarrow \left[-\nu^2 \left(\lambda_n^4 - \frac{K}{\tilde{a}} \right) \tilde{a} W_{2n}^{\mathrm{I}} - \tilde{a} W_{2n}^{\mathrm{III}} \right]_{\xi=b} = \left[-\nu^2 \left(\lambda_n^4 - \frac{K}{\tilde{a}} \right) \tilde{a} W_{1n}^{\mathrm{I}} - \tilde{a} W_{1n}^{\mathrm{III}} \right]_{\xi=b}, \quad (34b)$$

where $C = c/L$ denotes the dimensionless stiffness parameter of rotational springs.

Introducing (28) into (29)–(30) and (33)–(34), we obtain a matrix equation consisting of eight homogeneous algebraic equations for simply supported boundary conditions in the form

$$[G(\lambda_n)]\{\psi\} = \{0\}, \quad (35)$$

where $[G(\lambda_n)]$ is the matrix of natural frequency parameters λ_n and the term $\{\psi\}$ is the vector composed of eight unknown constants D_{ni}, $i = 1, 2, \dots, 8$. The nontrivial solution of the system (35) is obtained when the determinant of the system is equal to zero:

$$\det[G(\lambda_n)] = |G(\lambda_n)| = 0. \quad (36)$$

Solving these transcendent equations, we get the value of natural frequency and mode shape functions of the system for simply supported boundary conditions. Using the same methodology as in the previous case, substituting (28) into (31)–(32) and (33)–(34), we can obtain the frequency determinate for clamped-clamped boundary conditions in the form

$$|H(\lambda_n)| = 0. \quad (37)$$

The frequency determinants of the embedded nanotube for simply supported $|G(\lambda_n)|$ and clamped-clamped $|H(\lambda_n)|$ boundary conditions are given in the Appendix.

3. Numerical results and discussion

In order to perform a parametric study, we consider the following ranges of the dimensionless parameters: crack position $b = 0.25$–0.5, nonlocal parameter $\nu = 0$–0.6, crack severity $C = 0$–2 and stiffness of surrounding medium $K = 0$–1. These material and geometric parameters are adopted from [Loya et al. 2009]. In Tables 1 and 2, values of dimensionless natural frequencies of the cracked nanobeam are given for changes of nonlocal parameter ν, crack severity C and stiffness of surrounding medium K for various values of crack position b. Results for the simply supported boundary conditions are given in Table 1 while those for the clamped-clamped boundary conditions are shown in Table 2. By comparing the results obtained in this study with the results found in [Loya et al. 2009], it can be noticed that an excellent agreement is achieved for both cases of boundary conditions. Further, the influence of crack position on mode shape functions is presented in Figure 2. In addition, the effects of a longitudinal magnetic field and change in temperature on natural frequencies are shown in Figures 3 and 4.

		b = 0.5				b = 0.25			
K	ν	C = 0	C = 0.5	C = 1	C = 2	C = 0	C = 0.5	C = 1	C = 2
0	0	3.14159	2.63931	2.38319	2.09598	3.14159	2.82690	2.61743	2.34925
	0.2	2.89083	2.41902	2.17779	1.90983	2.89083	2.58446	2.37535	2.11337
	0.4	2.47903	2.06456	1.85242	1.61949	2.47903	2.19762	2.00246	1.76604
	0.6	2.15067	1.78664	1.60037	1.39708	2.15067	1.89756	1.72163	1.51254
0.5	0	3.14562	2.64609	2.39237	2.10943	3.14562	2.83242	2.62438	2.35883
	0.2	2.89599	2.42780	2.18979	1.92753	2.89599	2.59167	2.38463	2.12649
	0.4	2.48719	2.07862	1.87178	1.64815	2.48719	2.20930	2.01785	1.78830
	0.6	2.16313	1.80817	1.63003	1.44082	2.16313	1.91560	1.74562	1.54743
1	0	3.14962	2.65281	2.40145	2.12262	3.14962	2.83790	2.63127	2.36830
	0.2	2.90113	2.43649	2.20160	1.94475	2.90113	2.59882	2.39379	2.13937
	0.4	2.49528	2.09240	1.89055	1.67539	2.49528	2.22080	2.03289	1.80977
	0.6	2.17537	1.82895	1.65816	1.48091	2.17537	1.93314	1.76866	1.58012

Table 1. Values of the dimensionless natural frequency λ_n for the simply supported cracked nanobeam with different nonlocal parameter ν, crack severity C, stiffness of surrounding medium K and crack position b. (Compare to [Loya et al. 2009] especially for $K = 0$.)

From Table 1, it can be noticed that an increase in crack severity decreases the natural frequency parameter of the cracked nanobeam. Moreover, it can be observed that an increase in the nonlocal parameter causes a decrease in the natural frequency as expected. This implies that the small-scale effect reduces the rigidity of the system so that the nanobeam becomes "softer". An increase in the stiffness coefficients has very weak influence on natural frequency of the system, and it causes a slight increase

		b = 0.5				b = 0.25			
K	ν	C = 0	C = 0.5	C = 1	C = 2	C = 0	C = 0.5	C = 1	C = 2
0	0	4.73004	4.27235	4.10790	3.97023	4.73004	4.71675	4.71144	4.70681
	0.2	4.27661	3.79523	3.62032	3.47640	4.27661	4.26860	4.26418	4.25949
	0.4	3.59232	3.12694	2.96127	2.82852	3.59232	3.58948	3.58662	3.58104
	0.6	3.08370	2.66026	2.51211	2.39485	3.08370	3.08271	3.08094	3.06902
0.5	0	4.73122	4.27395	4.10970	3.97222	4.73122	4.71794	4.71263	4.70801
	0.2	4.27821	3.79751	3.62295	3.47937	4.27821	4.27021	4.26580	4.26110
	0.4	3.59501	3.13102	2.96607	2.83403	3.59501	3.59218	3.58932	3.58376
	0.6	3.08795	2.66688	2.51995	2.40390	3.08795	3.08697	3.08521	3.07334
1	0	4.73240	4.27555	4.11150	3.97422	4.73240	4.71913	4.71383	4.70920
	0.2	4.27981	3.79979	3.62558	3.48233	4.27981	4.27181	4.26740	4.26272
	0.4	3.59770	3.13509	2.97085	2.83950	3.5977	3.59488	3.59202	3.58647
	0.6	3.09219	2.67344	2.52773	2.41285	3.09219	3.09121	3.08946	3.07764

Table 2. Values of the dimensionless natural frequency λ_n for the clamped-clamped cracked nanobeam with different nonlocal parameter ν, crack severity C, stiffness of surrounding medium K and crack position b. (Compare to [Loya et al. 2009] especially for $K = 0$.)
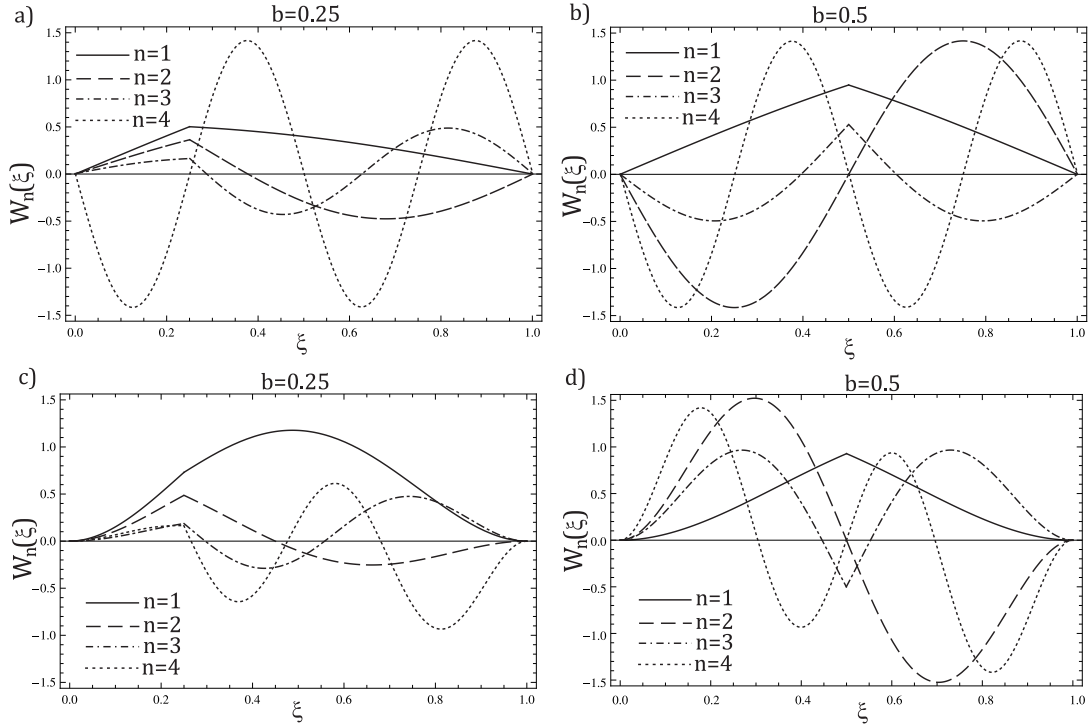
Figure 2. First four mode shapes of the simply supported nanobeam with (a) $b = 0.25$ and (b) $b = 0.5$ and of the clamped-clamped nanobeam with (c) $b = 0.25$ and (d) $b = 0.5$.

in the frequency as shown in Table 1. Also, it should be noted that when the crack severity is equal to zero we obtain natural frequencies of the embedded nanobeam without a crack. Comparing the natural frequencies from Table 1 for different crack positions, we can observe that, for a movement of crack position from the symmetric position at the middle of the nanobeam towards the boundaries, the natural frequency of the system decreases. This implies that the crack position has small influence on natural frequency when the crack is closer to the nanobeam boundaries.

In the case of clamped-clamped boundary conditions, we obtained higher values of natural frequencies due to the "stronger" constraints as shown in Table 2. Here, effects similar to those for the previous boundary conditions can be observed. An increase in crack severity as well as an increase in the nonlocal parameter causes a decrease in natural frequency while an increase in the medium's stiffness causes a slight increase in natural frequency. The $C = 0$ columns in Table 2 show natural frequencies of the clamped-clamped nanobeam without a crack. Considering the different crack positions in Table 2, we find that the natural frequency is higher for the case when the crack is closer to the boundaries while it decreases as the crack moves to the middle of the nanobeam.

It should be noted that the values of natural frequencies in this case reduce towards the values obtained in [Loya et al. 2009] when the longitudinal magnetic field, temperature change and stiffness of the elastic medium are equal to zero.

Mode shape functions of the cracked nanobeam for the first four vibration modes and two different boundary conditions and crack positions $b = 0.5$ and $b = 0.25$ are shown in Figure 2. For a simply
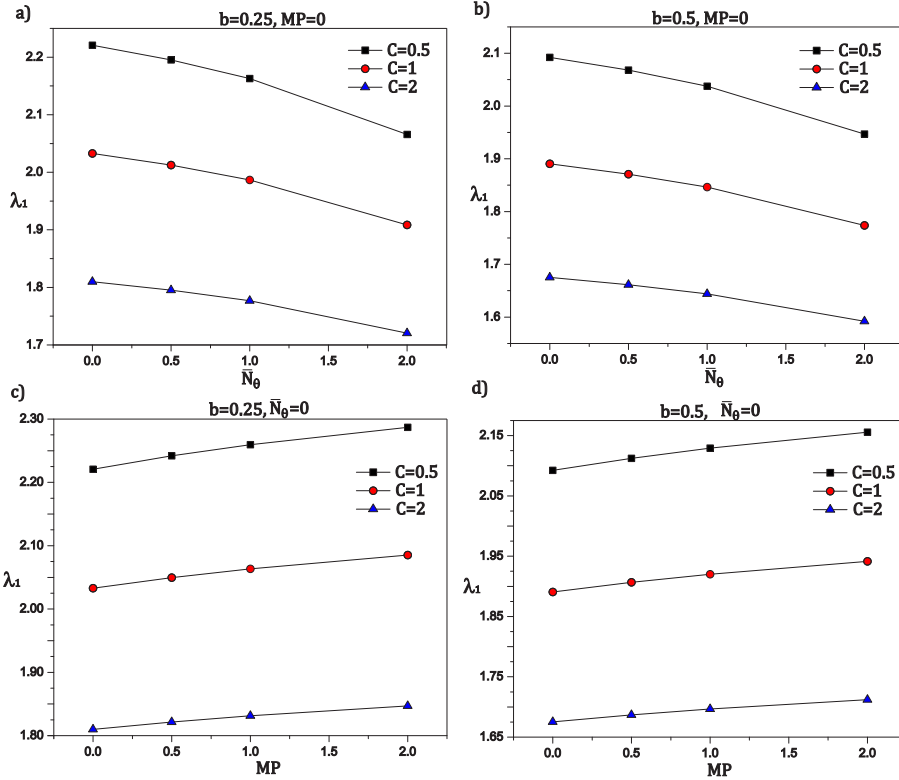
Figure 3. The first-mode natural frequency for a simply supported nanobeam with two crack positions.

supported nanobeam, in Figure 2a–b, we can observe that the differences of mode shape curves are localized near the crack position. When the crack is located at the middle of the nanobeam, we can notice the difference between symmetric and antisymmetric modes; i.e., differences of mode shape curves are visible only in the first and the third vibration mode and not for the second and the fourth mode. This is the case because the crack is located at the vibrational node, which is dependent on the mode number. It can be concluded that the crack does not affect the mode shape curve of the fourth vibration mode when the crack is located at a quarter of the length of the nanobeam (Figure 2a) and the second and fourth vibration modes when the crack is at the middle of the nanobeam (Figure 2b). In the next case, we analyze the clamped-clamped nanobeam in which a crack is located at $b = 0.25$ as shown in Figure 2c and at $b = 0.5$ in Figure 2d. As in the previous case, the crack causes changes in the mode shape functions. Also, it can be observed that deviations of mode shape curves allow us to detect surface defects in nanobeams and their control in the propagation.

Further, we examine the influence of thermal and magnetic field effects on the dimensionless natural frequency parameter of the cracked nanobeam embedded in an elastic medium. The following ranges of the dimensionless material and geometrical parameters of the cracked nanobeam are adopted: crack position $b = 0.25$–0.5, nonlocal parameter $\nu = 0.4$, crack severity $C = 0.5$–2, stiffness of surrounding medium $K = 1$, magnetic field parameter MP $= 0$–2 and thermal parameter $\bar{N}_\theta = 0$–2. In Figure 3, we
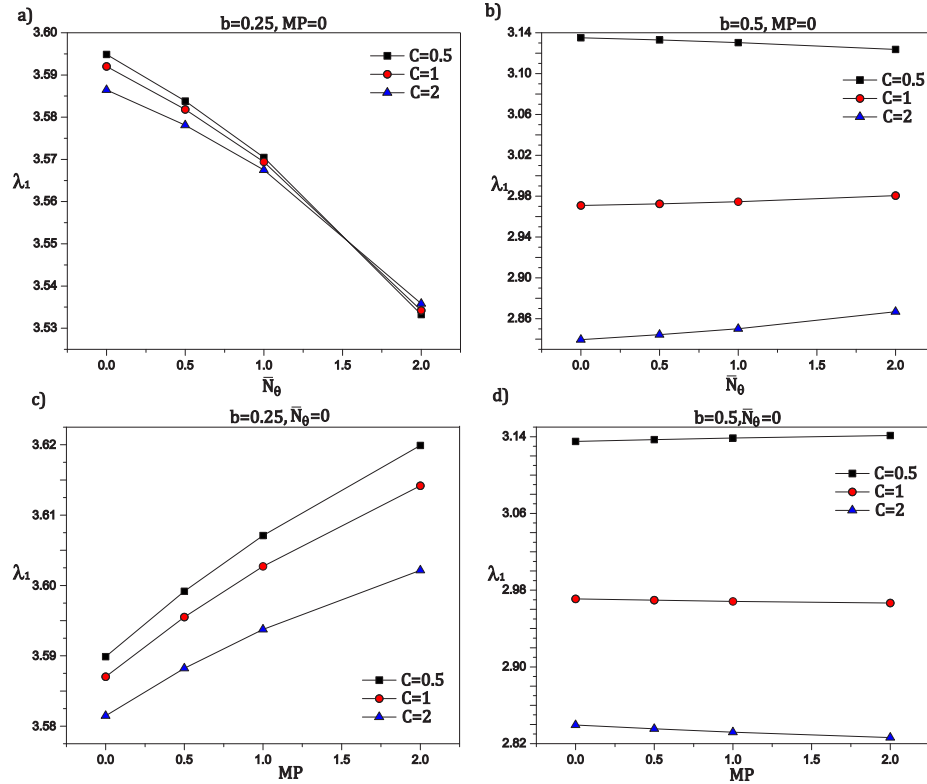
Figure 4. First natural frequency parameter for a clamped-clamped nanobeam with two crack positions.

plot the changes in the natural frequency parameter for different crack positions and simply supported boundary condition for two cases. In the first case, we consider the influence of thermal effect on the natural frequency parameter for MP = 0 (Figure 3a–b). Here, we can observe that an increase in the thermal coefficient causes a decrease in the natural frequency parameter for all values of crack severity and positions. This implies that the influence of thermal effect reduces the stiffness of the embedded nanobeam. From a physical point of view, the thermal parameter has damping effects on the vibration behavior of the cracked nanobeam. In the second case, we consider only the effect of the longitudinal magnetic field parameter on natural frequency as shown in Figure 3c–d. We can notice that an increase in the magnetic field parameter causes an increase in natural frequency for both cases of crack position in the nanobeam. Since an increase in the magnetic field parameter increases the rigidity of the system, it consequently increases the natural frequency parameter as well.

For further analysis of nonlocal vibration behavior of the cracked nanobeam embedded in an elastic medium, we will consider the systems with different crack positions and clamped-clamped boundary conditions. In addition, we adopt the same geometric and material parameters for the cracked nanobeam as in the previous case. Figure 4 shows changes in the natural frequency parameter for the clamped-clamped boundary condition case. It can be observed that for the crack position $b = 0.25$ there is no significant difference between natural frequencies with different crack severities. Further, it can be

noticed that an increase in the thermal coefficient causes a decrease in natural frequency for all cases. However, it can be noticed that the influence of crack stiffness is much smaller than in the case of the simply supported nanobeam. In addition, Figure 4b shows that for $b = 0.5$ the natural frequency slightly decreases for an increase in the thermal coefficient at the lowest value of crack severity but it slightly increases for an increase in the thermal coefficient when crack severities are higher. Figure 4c shows that for the crack position $b = 0.25$ natural frequencies are increasing for an increase in the magnetic field parameter in all cases. However, this is not the case when $b = 0.5$ as shown in Figure 4d. Here, it can be observed that the natural frequency slightly decreases for an increase of the magnetic field parameter at the lowest value of crack severity. However, it does not change for $C = 1$, and it slightly decreases for an increase in magnetic field parameter when $C = 2$. Finally, it should be noted that the system has a behavior similar to that of the case of the simply supported nanobeam for increased crack severity.

Analyzing the influence of external field parameters on the dynamic behavior of the cracked nanobeam structure, the following conclusion can be drawn. In the proposed model, the possibility of changing the natural frequency by variation of only external field parameters such as thermal and longitudinal magnetic field has a practical importance in design of NEMS devices. Choosing the proper magnitude of the external magnetic field in a certain range, it is possible to avoid the resonance state and increase the vibration amplitude at a given temperature. Moreover, this possibility allows us to control the crack propagation in a dynamic state of a nanostructure by controlling the total stiffness of a system. This study can be used as a starting point for the future investigation of vibration behavior of coupled nanobeams with cracks or in design procedures of nanodevices under the influence of various physical effects.

Conclusion

The main objective of this paper was to examine the influences of a magnetic field and thermal effects on the free vibration behavior of a cracked nanobeam. It can be concluded that natural frequency parameters of nanobeams are strongly influenced by the crack existence in the nanostructure. Various positions of the crack, different crack severities and different boundary conditions can change the values of natural frequencies or mode shape curves significantly. The influences of the two most commonly used boundary conditions in nanoengineering practice on the dynamic behavior of the embedded nanobeam were considered. It was found that the nanobeam with clamped-clamped boundary conditions has larger natural frequencies, and it is less sensitive to a change of parameters of the external magnetic field and temperature change. Thermal and longitudinal magnetic field effects on natural frequencies of cracked nanobeams were also investigated. Their influences are not negligible and can essentially change the vibration properties of nanobeams. This implies that the natural frequencies can be varied by a change in longitudinal magnetic field or temperature parameters without the necessity of changing the material and geometrical parameters of the nanosystem. These possibilities have great practical importance in the design of NEMS devices. A numerical parametric study was performed, and influences of various system parameters, such as the crack severities and position, nonlocality, longitudinal magnetic field, change in temperatures and stiffness of the elastic medium, on the natural frequency were investigated. It was found that the nonlocal parameter and crack severities have dampening effects on the natural frequency for both boundary conditions. Moreover, it can be seen that an increase in stiffness of the elastic medium leads to an increase in natural frequency, which implies an increase in the total stiffness of the system. In

addition, it is indicated that the influence of the crack position on the vibration mode is very important and significant for studying. The presented theoretical study can be very useful as a starting point in future analysis of dynamic and stability behaviors of more complex nanostructure systems with defects.

Appendix A

Let

$$X = v^2\left(\lambda_n^4 - \frac{K}{\tilde{a}}\right).$$

The frequency determinant in vibration analysis of the cracked nanobeam embedded in an elastic medium with simply supported boundary conditions is

$|G(\lambda_n)| =$

$$
\begin{vmatrix}
0 & 1 & 0 & 1 \\
0 & X+\alpha_n^2 & 0 & X-\beta_n^2 \\
\sinh(\alpha_n b) & \cosh(\alpha_n b) & \sin(\beta_n b) & \cos(\beta_n b) \\
C\alpha_n^2 \sinh(\alpha_n b)+\alpha_n \cosh(\alpha_n b) & C\alpha_n^2 \cosh(\alpha_n b)+\alpha_n \sinh(\alpha_n b) & -C\beta_n^2 \sin(\beta_n b)+\beta_n \cos(\beta_n b) & -C\beta_n^2 \cos(\beta_n b)-\beta_n \sin(\beta_n b) \\
(X+\alpha_n^2)\sinh(\alpha_n b) & (X+\alpha_n^2)\cosh(\alpha_n b) & (X-\beta_n^2)\sin(\beta_n b) & (X-\beta_n^2)\cos(\beta_n b) \\
(X\alpha_n+\alpha_n^3)\cosh(\alpha_n b) & (X\alpha_n+\alpha_n^3)\sinh(\alpha_n b) & (X\beta_n-\beta_n^3)\cos(\beta_n b) & -(X\beta_n+\beta_n^3)\sin(\beta_n b) \\
0 & 0 & 0 & 0 \\
0 & 0 & 0 & 0
\end{vmatrix}
$$

$$
\begin{vmatrix}
0 & 0 & 0 & 0 \\
0 & 0 & 0 & 0 \\
-\sinh(\alpha_n b) & -\cosh(\alpha_n b) & -\sin(\beta_n b) & -\cos(\beta_n b) \\
-\alpha_n \cosh(\alpha_n b) & -\alpha_n \sinh(\alpha_n b) & -\beta_n \cos(\beta_n b) & \beta_n \sin(\beta_n b) \\
-(X+\alpha_n^2)\sinh(\alpha_n b) & -(X+\alpha_n^2)\cosh(\alpha_n b) & -(X-\beta_n^2)\sin(\beta_n b) & -(X-\beta_n^2)\cos(\beta_n b) \\
-(X\alpha_n+\alpha_n^3)\cosh(\alpha_n b) & -(X\alpha_n+\alpha_n^3)\sinh(\alpha_n b) & -(X\beta_n-\beta_n^3)\cos(\beta_n b) & (X\beta_n+\beta_n^3)\sin(\beta_n b) \\
\sinh(\alpha_n) & \cosh(\alpha_n) & \sin(\beta_n) & \cos(\beta_n) \\
(X+\alpha_n^2)\sinh(\alpha_n) & (X+\alpha_n^2)\cosh(\alpha_n) & (X-\beta_n^2)\sin(\beta_n) & (X-\beta_n^2)\cos(\beta_n)
\end{vmatrix}.
$$

The frequency determinant in vibration analysis of the cracked nanobeam embedded in an elastic medium with clamped-clamped boundary conditions is

$|H(\lambda_n)| =$

$$
\begin{vmatrix}
0 & 1 & 0 & 1 \\
\alpha_n & 0 & \beta_n & 0 \\
\sinh(\alpha_n b) & \cosh(\alpha_n b) & \sin(\beta_n b) & \cos(\beta_n b) \\
C\alpha_n^2 \sinh(\alpha_n b)+\alpha_n \cosh(\alpha_n b) & C\alpha_n^2 \cosh(\alpha_n b)+\alpha_n \sinh(\alpha_n b) & -C\beta_n^2 \sin(\beta_n b)+\beta_n \cos(\beta_n b) & -C\beta_n^2 \cos(\beta_n b)-\beta_n \sin(\beta_n b) \\
(X+\alpha_n^2)\sinh(\alpha_n b) & (X+\alpha_n^2)\cosh(\alpha_n b) & (X-\beta_n^2)\sin(\beta_n b) & (X-\beta_n^2)\cos(\beta_n b) \\
(X\alpha_n+\alpha_n^3)\cosh(\alpha_n b) & (X\alpha_n+\alpha_n^3)\sinh(\alpha_n b) & (X\beta_n-\beta_n^3)\cos(\beta_n b) & -(X\beta_n+\beta_n^3)\sin(\beta_n b) \\
0 & 0 & 0 & 0 \\
0 & 0 & 0 & 0
\end{vmatrix}
$$

$$
\begin{vmatrix}
0 & 0 & 0 & 0 \\
0 & 0 & 0 & 0 \\
-\sinh(\alpha_n b) & -\cosh(\alpha_n b) & -\sin(\beta_n b) & -\cos(\beta_n b) \\
-\alpha_n \cosh(\alpha_n b) & -\alpha_n \sinh(\alpha_n b) & -\beta_n \cos(\beta_n b) & \beta_n \sin(\beta_n b) \\
-(X+\alpha_n^2)\sinh(\alpha_n b) & -(X+\alpha_n^2)\cosh(\alpha_n b) & -(X-\beta_n^2)\sin(\beta_n b) & -(X-\beta_n^2)\cos(\beta_n b) \\
-(X\alpha_n+\alpha_n^3)\cosh(\alpha_n b) & -(X\alpha_n+\alpha_n^3)\sinh(\alpha_n b) & -(X\beta_n-\beta_n^3)\cos(\beta_n b) & (X\beta_n+\beta_n^3)\sin(\beta_n b) \\
\sinh(\alpha_n) & \cosh(\alpha_n) & \sin(\beta_n) & \cos(\beta_n) \\
\alpha_n \cosh(\alpha_n) & \alpha_n \sinh(\alpha_n) & \beta_n \cos(\beta_n) & -\beta_n \sin(\beta_n)
\end{vmatrix}.
$$

The vector $\{\psi\}$ is composed of eight unknown constants D_{ni}, $i = 1, 2, \ldots, 8$, defined as

$$\{\psi\}^T = \{D_{n1}, D_{n2}, D_{n3}, D_{n4}, D_{n5}, D_{n6}, D_{n7}, D_{n8}\}^T.$$

References

[A. Haghshenas and Arani 2013] A. A. Haghshenas and A. G. Arani, "Nonlocal vibration of a piezoelectric polymeric nanoplate carrying nanoparticle via Mindlin plate theory", *Proc. Inst. Mech. Eng. C, J. Mech. Eng. Sci.* **228**:5 (2013), 907–920.

[Alper and Hamad-Schifferli 2010] J. Alper and K. Hamad-Schifferli, "Effect of ligands on thermal dissipation from gold nanorods", *Langmuir* **26**:6 (2010), 3786–3789.

[Ansari et al. 2012] R. Ansari, R. Gholami, and M. A. Darabi, "A nonlinear Timoshenko beam formulation based on strain gradient theory", *J. Mech. Mater. Struct.* **7**:2 (2012), 195–211.

[Arani et al. 2013] A. H. G. Arani, M. J. Maboudi, A. G. Arani, and S. Amir, "2D-Magnetic field and biaxiall in-plane pre-load effects on the vibration of double bonded orthotropic graphene sheets", *J. Solid Mech.* **5**:2 (2013), 193–205.

[Batra et al. 2007] R. C. Batra, M. Porfiri, and D. Spinello, "Review of modeling electrostatically actuated microelectromechanical systems", *Smart Mater. Struct.* **16**:6 (2007), R23.

[Belytschko et al. 2002] T. Belytschko, S. P. Xiao, G. C. Schatz, and R. S. Ruoff, "Atomistic simulations of nanotube fracture", *Phys. Rev. B* **65**:23 (2002), 235430.

[Benzair et al. 2008] A. Benzair, A. Tounsi, A. Besseghier, H. Heireche, N. Moulay, and L. Boumia, "The thermal effect on vibration of single-walled carbon nanotubes using nonlocal Timoshenko beam theory", *J. Phys. D Appl. Phys.* **41**:22 (2008), 225404.

[Bershtein et al. 2002] V. A. Bershtein, L. M. Egorova, P. N. Yakushev, P. Pissis, P. Sysel, and L. Brozova, "Molecular dynamics in nanostructured polyimide–silica hybrid materials and their thermal stability", *J. Polym. Sci. B Polym. Phys.* **40**:10 (2002), 1056–1069.

[Charlier 2002] J.-C. Charlier, "Defects in carbon nanotubes", *Acc. Chem. Res.* **35**:12 (2002), 1063–1069.

[Eringen 1972] A. C. Eringen, "Linear theory of nonlocal elasticity and dispersion of plane waves", *Int. J. Eng. Sci.* **10**:5 (1972), 425–435.

[Eringen 1983] A. C. Eringen, "On differential equations of nonlocal elasticity and solutions of screw dislocation and surface waves", *J. Appl. Phys.* **54**:9 (1983), 4703–4710.

[Fernández-Sáez and Navarro 2002] J. Fernández-Sáez and C. Navarro, "Fundamental frequency of cracked beams in bending vibrations: An analytical approach", *J. Sound Vib.* **256**:1 (2002), 17–31.

[Fernández-Sáez et al. 1999] J. Fernández-Sáez, L. Rubio, and C. Navarro, "Approximate calculation of the fundamental frequency for bending vibrations of cracked beams", *J. Sound Vib.* **225**:2 (1999), 345–352.

[Firouz-Abadi and Hosseinian 2012] R. D. Firouz-Abadi and A. R. Hosseinian, "Resonance frequencies and stability of a current-carrying suspended nanobeam in a longitudinal magnetic field", *Theor. Appl. Mech. Lett.* **2**:3 (2012), 031012.

[Gómez-Navarro et al. 2008] C. Gómez-Navarro, M. Burghard, and K. Kern, "Elastic properties of chemically derived single graphene sheets", *Nano Lett.* **8**:7 (2008), 2045–2049.

[Hasheminejad et al. 2011] B. S. M. Hasheminejad, B. Gheshlaghi, Y. Mirzaei, and S. Abbasion, "Free transverse vibrations of cracked nanobeams with surface effects", *Thin Solid Films* **519**:8 (2011), 2477–2482.

[Hosseini-Hashemi et al. 2014] S. Hosseini-Hashemi, I. Nahas, M. Fakher, and R. Nazemnezhad, "Surface effects on free vibration of piezoelectric functionally graded nanobeams using nonlocal elasticity", *Acta Mech.* **225**:6 (2014), 1555–1564.

[Hsieh et al. 2006] J.-Y. Hsieh, J.-M. Lu, M.-Y. Huang, and C.-C. Hwang, "Theoretical variations in the Young's modulus of single-walled carbon nanotubes with tube radius and temperature: A molecular dynamics study", *Nanotechnology* **17**:15 (2006), 3920.

[Jam et al. 2012] J. E. Jam, Y. Mirzaei, B. Gheshlaghi, and R. Avazmohammadi, "Size-dependent free vibration analysis of infinite nanotubes using elasticity theory", *J. Mech. Mater. Struct.* **7**:2 (2012), 137–144.

[Jensen 1999] P. Jensen, "Growth of nanostructures by cluster deposition: Experiments and simple models", *Rev. Mod. Phys.* **71**:5 (1999), 1695–1735.

[Karličić et al. 2014] D. Karličić, T. Murmu, M. Cajić, P. Kozić, and S. Adhikari, "Dynamics of multiple viscoelastic carbon nanotube based nanocomposites with axial magnetic field", *J. Appl. Phys.* **115**:23 (2014), 234303.

[Ke and Wang 2012] L.-L. Ke and Y.-S. Wang, "Thermoelectric-mechanical vibration of piezoelectric nanobeams based on the nonlocal theory", *Smart Mater. Struct.* **21**:2 (2012), 025018.

[Kiani 2012] K. Kiani, "Magneto–thermo–elastic fields caused by an unsteady longitudinal magnetic field in a conducting nanowire accounting for eddy-current loss", *Mater. Chem. Phys.* **136**:2–3 (2012), 589–598.

[Kiani 2014a] K. Kiani, "Free vibration of conducting nanoplates exposed to unidirectional in-plane magnetic fields using nonlocal shear deformable plate theories", *Physica E* **57** (2014), 179–192.

[Kiani 2014b] K. Kiani, "Vibration and instability of a single-walled carbon nanotube in a three-dimensional magnetic field", *J. Phys. Chem. Solids* **75**:1 (2014), 15–22.

[Kisa and Gurel 2006] M. Kisa and M. A. Gurel, "Modal analysis of multi-cracked beams with circular cross section", *Eng. Fract. Mech.* **73**:8 (2006), 963–977.

[Kozić et al. 2014] P. Kozić, R. Pavlović, and D. Karličić, "The flexural vibration and buckling of the elastically connected parallel-beams with a Kerr-type layer in between", *Mech. Res. Commun.* **56** (2014), 83–89.

[Li et al. 2011] S. Li, H. J. Xie, and X. Wang, "Dynamic characteristics of multi-walled carbon nanotubes under a transverse magnetic field", *Bull. Mater. Sci.* **34**:1 (2011), 45–52.

[Loya et al. 2006] J. A. Loya, L. Rubio, and J. Fernández-Sáez, "Natural frequencies for bending vibrations of Timoshenko cracked beams", *J. Sound Vib.* **290**:3–5 (2006), 640–653.

[Loya et al. 2009] J. Loya, J. López-Puente, R. Zaera, and J. Fernández-Sáez, "Free transverse vibrations of cracked nanobeams using a nonlocal elasticity model", *J. Appl. Phys.* **105**:4 (2009), 044309.

[Loya et al. 2014] J. A. Loya, J. Aranda-Ruiz, and J. Fernández-Sáez, "Torsion of cracked nanorods using a nonlocal elasticity model", *J. Phys. D Appl. Phys.* **47**:11 (2014), 115304.

[Martín et al. 2012] J. Martín, M. Hernández-Vélez, O. de Abril, C. Luna, A. Munoz-Martin, M. Vázquez, and C. Mijangos, "Fabrication and characterization of polymer-based magnetic composite nanotubes and nanorods", *Eur. Polym. J.* **48**:4 (2012), 712–719.

[Meyer et al. 2007] J. C. Meyer, A. K. Geim, M. I. Katsnelson, K. S. Novoselov, T. J. Booth, and S. Roth, "The structure of suspended graphene sheets", *Nature* **446**:7131 (2007), 60–63.

[Murmu and Pradhan 2009] T. Murmu and S. C. Pradhan, "Thermo-mechanical vibration of a single-walled carbon nanotube embedded in an elastic medium based on nonlocal elasticity theory", *Comput. Mater. Sci.* **46**:4 (2009), 854–859.

[Murmu and Pradhan 2010] T. Murmu and S. C. Pradhan, "Thermal effects on the stability of embedded carbon nanotubes", *Comput. Mater. Sci.* **47**:3 (2010), 721–726.

[Murmu et al. 2013] T. Murmu, M. A. McCarthy, and S. Adhikari, "In-plane magnetic field affected transverse vibration of embedded single-layer graphene sheets using equivalent nonlocal elasticity approach", *Compos. Struct.* **96** (2013), 57–63.

[Murmu et al. 2014] T. Murmu, S. Adhikari, and M. A. McCarthy, "Axial vibration of embedded nanorods under transverse magnetic field effects via nonlocal elastic continuum theory", *J. Comput. Theor. Nanosci.* **11**:5 (2014), 1230–1236.

[Narendar et al. 2012] S. Narendar, S. S. Gupta, and S. Gopalakrishnan, "Wave propagation in single-walled carbon nanotube under longitudinal magnetic field using nonlocal Euler–Bernoulli beam theory", *Appl. Math. Model.* **36**:9 (2012), 4529–4538.

[Niyogi et al. 2006] S. Niyogi, E. Bekyarova, M. E. Itkis, J. L. McWilliams, M. A. Hamon, and R. C. Haddon, "Solution properties of graphite and graphene", *J. Amer. Chem. Soc.* **128**:24 (2006), 7720–7721.

[Park et al. 2005] S. H. Park, J. S. Kim, J. H. Park, J. S. Lee, Y. K. Choi, and O. M. Kwon, "Molecular dynamics study on size-dependent elastic properties of silicon nanocantilevers", *Thin Solid Films* **492**:1–2 (2005), 285–289.

[Popov et al. 2007] A. M. Popov, E. Bichoutskaia, Y. E. Lozovik, and A. S. Kulish, "Nanoelectromechanical systems based on multi-walled nanotubes: Nanothermometer, nanorelay, and nanoactuator", *Phys. Status Solidi A* **204**:6 (2007), 1911–1917.

[Reddy and Pang 2008] J. N. Reddy and S. D. Pang, "Nonlocal continuum theories of beams for the analysis of carbon nanotubes", *J. Appl. Phys.* **103**:2 (2008), 023511.

[Roostai and Haghpanahi 2014] H. Roostai and M. Haghpanahi, "Vibration of nanobeams of different boundary conditions with multiple cracks based on nonlocal elasticity theory", *Appl. Math. Model.* **38**:3 (2014), 1159–1169.

[Sammalkorpi et al. 2004] M. Sammalkorpi, A. Krasheninnikov, A. Kuronen, K. Nordlund, and K. Kaski, "Mechanical properties of carbon nanotubes with vacancies and related defects", *Phys. Rev. B* **70**:24 (2004), 245416.

[Schniepp et al. 2006] H. C. Schniepp, J.-L. Li, M. J. McAllister, H. Sai, M. Herrera-Alonso, D. H. Adamson, R. K. Prud'homme, R. Car, D. A. Saville, and I. A. Aksay, "Functionalized single graphene sheets derived from splitting graphite oxide", *J. Phys. Chem. B* **110**:17 (2006), 8535–8539.

[Torabi and Dastgerdi 2012] K. Torabi and J. N. Dastgerdi, "An analytical method for free vibration analysis of Timoshenko beam theory applied to cracked nanobeams using a nonlocal elasticity model", *Thin Solid Films* **520**:21 (2012), 6595–6602.

[Wei and Wang 2004] L. Wei and Y.-N. Wang, "Electromagnetic wave propagation in single-wall carbon nanotubes", *Phys. Lett. A* **333**:3–4 (2004), 303–309.

[Wu et al. 2005] B. Wu, A. Heidelberg, and J. J. Boland, "Mechanical properties of ultrahigh-strength gold nanowires", *Nat. Mater.* **4**:7 (2005), 525–529.

[Xie et al. 2000] S. Xie, W. Li, Z. Pan, B. Chang, and L. Sun, "Mechanical and physical properties on carbon nanotube", *J. Phys. Chem. Solids* **61**:7 (2000), 1153–1158.

[Xing et al. 2004] Y. J. Xing, Z. H. Xi, X. D. Zhang, J. H. Song, R. M. Wang, J. Xu, Z. Q. Xue, and D. P. Yu, "Nanotubular structures of zinc oxide", *Solid State Comm.* **129**:10 (2004), 671–675.

[Yang and Chen 2008] J. Yang and Y. Chen, "Free vibration and buckling analyses of functionally graded beams with edge cracks", *Compos. Struct.* **83**:1 (2008), 48–60.

[Youssef and Elsibai 2011] H. M. Youssef and K. A. Elsibai, "Vibration of gold nanobeam induced by different types of thermal loading—a state-space approach", *Nanoscale Microscale Thermophys. Eng.* **15**:1 (2011), 48–69.

[Yum and Yu 2006] K. Yum and M.-F. Yu, "Measurement of wetting properties of individual boron nitride nanotubes with the Wilhelmy method using a nanotube-based force sensor", *Nano Lett.* **6**:2 (2006), 329–333.

[Zhang et al. 2005] S. Zhang, S. L. Mielke, R. Khare, D. Troya, R. S. Ruoff, G. C. Schatz, and T. Belytschko, "Mechanics of defects in carbon nanotubes: Atomistic and multiscale simulations", *Phys. Rev. B* **71**:11 (2005), 115403.

[Zhang et al. 2008] Y. Q. Zhang, X. Liu, and J. H. Zhao, "Influence of temperature change on column buckling of multiwalled carbon nanotubes", *Phys. Lett. A* **372**:10 (2008), 1676–1681.

[Zhou and Shi 2003] L. G. Zhou and S.-Q. Shi, "Formation energy of Stone–Wales defects in carbon nanotubes", *Appl. Phys. Lett.* **83**:6 (2003), 1222–1224.

DANILO KARLIČIĆ: danilo.karlicic@masfak.ni.ac.rs
Faculty of Mechanical Engineering, University of Niš, Aleksandra Medvedeva 14, 18000 Niš, Serbia

DRAGAN JOVANOVIĆ: jdragan@masfak.ni.ac.rs
Faculty of Mechanical Engineering, University of Niš, Aleksandra Medvedeva 14, 18000 Niš, Serbia

PREDRAG KOZIĆ: kozicp@yahoo.com
Faculty of Mechanical Engineering, University of Niš, Aleksandra Medvedeva 14, 18000 Niš, Serbia

MILAN CAJIĆ: caja84@gmail.com
Mathematical Institute of the Serbian Academy of Sciences and Arts, Kneza Mihaila 36, 11001 Belgrade, Serbia

JOURNAL OF MECHANICS OF MATERIALS AND STRUCTURES

msp.org/jomms

Founded by Charles R. Steele and Marie-Louise Steele

Cover photo: Ev Shafrir